JACS
JOURNAL OF THE AMERICAN CHEMICAL SOCIETY
Article
pubs.acs.org/JACS

Catalytic Light-Driven Generation of Hydrogen from Water by Iron Dithiolene Complexes

Hongjin Lv, T. Purnima A. Ruberu, Valerie E. Fleischauer, William W. Brennessel, Michael L. Neidig, and Richard Eisenberg*

Department of Chemistry, University of Rochester, Rochester, New York 14627, United States

Supporting Information

ABSTRACT: The development of active, robust systems for light-driven hydrogen production from aqueous protons based on catalysts and light absorbers composed solely of earth abundant elements remains a challenge in the development of an artificial photosynthetic system for water splitting. Herein, we report the synthesis and characterization of four closely related Fe bis(benzenedithiolate) complexes that exhibit catalytic activity for hydrogen evolution when employed in systems with water-soluble CdSe QDs as photosensitizer and ascorbic acid as a sacrificial electron source under visible light irradiation (520 nm). The complex with the most electron-donating dithiolene ligand exhibits the highest activity, the overall order of activity correlating with the reduction potential of the formally Fe(III) dimeric dianions. Detailed studies of the effect of different capping agents and the extent of surface coverage of these capping agents on the CdSe QD surfaces reveal that they affect system activity and provide insight into the continued development of such systems containing QD light absorbers and molecular catalysts for H_2 formation.

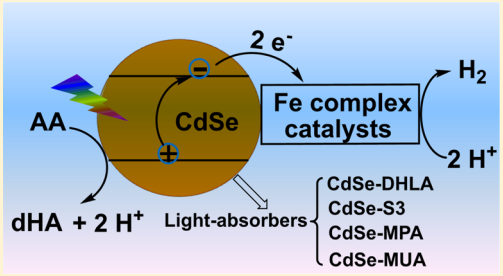

INTRODUCTION

Visible light-driven water splitting into H_2 and O_2 via artificial photosynthesis (AP) is a central theme of solar fuel production that will prove critically important in light of projected increases in global energy demand and the need to minimize carbon emissions with regard to global climate change.[1−5] In light of the intrinsic complexity of water splitting (a four-electron, four-proton redox reaction), AP systems for this energy-storing reaction are generally studied in terms of two half-reactions: water oxidation to O_2 and aqueous proton reduction to H_2. The light-driven reduction of water to H_2 by molecularly based systems has been known since the late 1970s when researchers developed systems comprising $[Ru(bpy)_3]^{2+}$ and/or its derivatives as light absorbers in the presence of a suitable catalyst such as Pt, an electron mediator, and a sacrificial electron.[6−9] In recent years, extensive efforts have been made to replace precious metal components of aqueous proton reduction systems with more active and durable constituents made solely of earth-abundant elements. For possible catalysts in homogeneous water reduction systems, the focus has been on potentially redox active transition metal complexes of elements such as iron,[10−13] cobalt,[14−19] nickel,[20−26] and molybdenum.[27,28] Despite extensive experimental investigations and mechanistic studies of systems containing these water reduction catalysts (WRCs), many of them have been found to suffer from low activity and/or photoinstability due to decomposition of the chromophore, or catalyst degradation due to structural instability.[29−31] While significant improvements have been reported,[16,18−20,22−25] the challenge still remains for an active and robust sunlight-driven system for hydrogen production from water. The development of new, efficient earth-abundant transition metal catalysts and photostable light-absorbers remains part of that challenge.

Significant progress has been made locally and elsewhere within the past few years regarding both the design of novel catalysts and photostable light-absorbers.[22,32−34] In these studies, water-soluble cadmium selenide (CdSe) semiconductor quantum dots (QDs) have been used as an alternative chromophore for visible-light-driven hydrogen production.[35−41] Compared with molecular light absorbers such as $Ru(bpy)_3^{2+}$ and the organic dyes Fluorescein and Eosin Y, semiconductor QDs have advantages of superior photostability, tunable redox potentials, large absorption cross sections across the visible spectrum, and the propensity for photoinduced electron transfer for catalysis.[35,36,39,42]

With respect to the development of novel and stable catalysts, one interesting family of WRCs are metal dithiolene complexes,[16,32,43] in which the dithiolene ligands can undergo reversible electron transfers with minimal structural perturbations and are resistant toward hydrogenation.[44,45] These attractive properties make them proper candidates for multi-electron-transfer catalysis as in proton reduction to H_2. To date, the Co-based bis(benzenedithiolate) (bdt) complexes and related Ni systems have demonstrated promising activity toward both light-driven and electrocatalytic hydrogen production,[16,32,33,43] but Fe-based dithiolene complexes as catalysts for hydrogen evolution have been largely unexplored.[46,47] Given the fact that Fe_2S_2 or $FeNiS_2$ clusters are the active sites of [FeFe]

Received: May 16, 2016
Published: September 1, 2016

DOI: 10.1021/jacs.6b05040
J. Am. Chem. Soc. 2016, 138, 11654−11663

or [FeNi] hydrogenases (the most efficient catalysts for hydrogen uptake and proton reduction),[48−51] a number of recent studies have been reported that use semiconductor nanoparticles as light-absorbers and [FeFe] hydrogenase or their mimics as the catalysts. For example, Dukovic, King and co-workers reported systems using CdS-MPA nanorods (MPA = the capping agent 3-mercaptopropionic acid) and [FeFe]-hydrogenase I that promote light-driven H_2 production with a turnover frequency (TOF) of 380−900 s^{-1} upon irradiation at 405 nm.[37] In another study, Wu and co-workers have described the assembly of an [FeFe]-hydrogenase mimic with CdSe QDs using an interface-directed approach, with resultant activity in the photogeneration of H_2 of 8781 turnovers (TONs) and an initial turnover frequency (TOF) of 596 h^{-1} under visible light irradiation.[40b] On the basis of these observations and work done locally on the light-driven generation H_2 using Co and Ni complexes of redox active unsaturated ligands as catalysts,[16,32,33] related iron complexes containing 1,2-dithiolene ligands appeared to be potentially interesting candidates as cost-effective catalysts for hydrogen production. An important clue to potential activity was provided nearly 25 years ago when Sellmann and co-workers reported that the complex $[Fe^{(II)}(bdt)_2]^{2-}$ catalyzed proton reduction to H_2 but the process was stoichiometric and not shown to be catalytic.[46]

In this context, we report here the synthesis and characterization of four closely related Fe dithiolene complexes and their catalytic hydrogen evolution activity when using water-soluble CdSe QDs as photosensitizer and ascorbic acid as the sacrificial electron donor. Detailed studies on the influence of different capping agents and the extent of surface coverage of CdSe QDs by these capping agents also yield insight into the continuing development of highly robust and superior efficient catalytic systems for solar energy utilization.

EXPERIMENTAL SECTION

Materials. All starting chemicals and solvents for syntheses, characterization, and catalytic studies were purchased from commercial sources and were used as received without further purification unless otherwise noted. The solvents for syntheses were dried using 4 Å molecular sieves before use. For photocatalytic hydrogen evolution experiments, deionized water and ethanol (1/1 volume ratio) was used. Two water-solubilizing capping agents, dihydrolopic acid (DHLA) and 3-mercapto-2,2-bis(mercaptomethyl)propanoic acid (S3), were synthesized following literature methods.[32,52] Other water-solubilizing capping agents, 3-mercaptopropionic acid (MPA) and 11-mercaptoundecanoic acid (MUA), were purchased from Aldrich and used as received. The tri-*n*-octylphosphine oxide-capped CdSe (CdSe-TOPO) QDs were prepared using slightly modified procedures to that reported previously,[53] and the water-soluble CdSe nanocrystals (CdSe-DHLA, CdSe-S3, CdSe-MPA, and CdSe-MUA) were synthesized through ligand exchange reactions in methanol under N_2 atmosphere (see experimental details in the SI).[22,32,39,41]

Instrumentation. The ^{1}H NMR spectra were recorded on a Bruker Avance 400-MHz spectrometer and referenced to residual proton resonances of the deuterated solvents. The magnetic susceptibility measurements for all four Fe complexes were performed by the Evans Method[54] using an NMR tube with a coaxial insert. The NMR tube contains a THF-d_8 solution of the Fe-complex with 2% reference substance (*t*-butanol) and the coaxial insert contains only the THF-d_8 solvent and reference substance. The difference in chemical shift of the reference compound caused by the paramagnetic compounds was recorded and used for effective magnetic moment calculation. UV−vis spectra were recorded on a Cary 60 UV/vis spectrophotometer, using a 1 cm or 2 mm path length quartz cuvette. The UV−vis spectra of all Fe-dithiolene complexes were recorded in CH_3CN solution; the spectra of CdSe-TOPO QDs were measured in hexane and those of water-soluble CdSe QDs were performed in water. Elemental analyses were performed using a PerkinElmer 2400 Series II Analyzer. Cyclic Voltammetry (CV) measurements were performed with a CHI 680D potentiostat at room temperature under Ar atmosphere, using a one-compartment cell with a glassy carbon working electrode (3 mm diameter), Pt auxiliary electrode, and saturated calomel reference electrode (SCE). Tetrabutylammonium hexafulorophosphate ($TBAPF_6$) was used as supporting electrolyte for all CV measurements.

*Synthesis of $(NBu_4)_2[Fe(bdt)_2]_2$ (**1**).* In a Schlenk flask, 1,2-benzenedithiol (237.1 mg, 1.67 mmol) and NaOMe (185 mg, 3.42 mmol) were dissolved in 25 mL of dry MeOH under an N_2 atmosphere and allowed to stir at room temperature for 10 min. To this solution, a degassed mixture of $Fe(NO_3)_3{\cdot}9H_2O$ (343 mg, 0.85 mmol) in MeOH (5 mL) was added dropwise. The solution was stirred for 1 h at room temperature while the color became black-red. To this solution, a solution of NBu_4Br (275.2 mg, 0.85 mmol) in 5 mL of MeOH was added, then the solution was allowed to stir at room temperature overnight under an air atmosphere. After reaction, the solvent was completely removed under vacuum, and a black-red precipitate formed. The black-red precipitate was extracted using tetrahydrofuran (3 × 15 mL); the combined organic layer was filtered and dried under rotary evaporator to obtain a pure black-red solid (330 mg, 67% yield). Crystals for X-ray diffraction were grown by diffusion of diethyl ether to a concentrated solution of $(NBu_4)_2[Fe(bdt)_2]_2$ in dichloromethane. Elemental analyses: Calcd: C, 58.11; H, 7.66; N, 2.42; Found: C, 58.34; H, 7.93; N, 2.57.

*Synthesis of $(NBu_4)_2[Fe(tdt)_2]_2$ (**2**).* This complex was synthesized in a procedure analogous to that described for $(NBu_4)_2[Fe(bdt)_2]_2$ except that toluene-3,4-dithiol (261 mg, 1.67 mmol) was used. The yield is 366 mg (71%). Crystals for X-ray diffraction were grown by diffusion of diethyl ether to a concentrated solution of $(NBu_4)_2[Fe(tdt)_2]_2$ in dichloromethane. Elemental analyses: Calcd: C, 59.37; H, 7.97; N, 2.31; Found: C, 58.84; H, 7.93; N, 2.12.

*Synthesis of $(NBu_4)_2[Fe(dcbdt)_2]_2$ (**3**).* This complex was synthesized in a procedure analogous to that described for $(NBu_4)_2[Fe(bdt)_2]_2$ except that 3,6-dichloro-1,2-benzenedithiol (352.5 mg, 1.67 mmol) was used. The yield is 396 mg (65%). Crystals for X-ray diffraction were grown by diffusion of diethyl ether to a concentrated solution of $(NBu_4)_2[Fe(bdt\text{-}Cl_2)_2]_2$ in dichloromethane. Elemental analyses Calcd: C, 46.93; H, 5.62; N, 1.95; Found: C, 46.28; H, 5.38; N, 2.02.

Synthesis of 3,4,5,6-Tetrachlorobenzene-1,2-dithiol (tcbdt). 3,4,5,6-Tetrachloro-benzene-1,2-dithiol (tcbdt) was prepared following a slightly modified literature method.[55] In a typical experiment, a mixture of hexachlorobenzene (25 g), iron powder (2.57 g), NaHS (19 g), and sulfur (0.22 g) in 90 mL dimethylformamide (DMF) was refluxed for 14 h under N_2 atmosphere. After reaction, the mixture was cooled to room temperature and diluted with NaOH solution (0.375 M, 100 mL). The black crude tetrachlorobenzenedithiolate iron complex was obtained under vacuum suction and dried at room temperature overnight. ***Caution!*** *Hexachlorobenzene is considered to be a probable human carcinogen and dangerous for the environment; make sure this chemical is handled with personal protective equipment!* Then, the crude tetrachlorobenzenedithiol-iron complex (~32 g) was dispersed in 180 mL warm methanol, and to this mixture was added a solution of zinc oxide (10.5 g) and NaOH (27 g) in 200 mL water at 50 °C. The resulting mixture was refluxed at around 75 °C for 1.5 h; the solution was filtered and the filtrate was added to a solution of concentrated sulfuric acid (102 mL) in 350 mL water. After cooling to room temperature, the yellow precipitate was filtered off, washed with deionized water for three times and dried under vacuum overnight. The yield of this pale yellow 3,4,5,6-tetrachlorobenzene-1,2-dithiol was 4.55 g (18.5%).

*Synthesis of $(NBu_4)_2[Fe(tcbdt)_2]_2$ (**4**).* This complex was synthesized in a procedure analogous to that described for $(NBu_4)_2[Fe(bdt)_2]_2$ except that 3,4,5,6-tetrachlorobenzene-1,2-dithiol (280 mg, 1 mmol), NaOMe (108 mg, 2 mmol), $Fe(NO_3)_3{\cdot}9H_2O$ (202 mg, 0.5 mmol), and NBu_4Br (161 mg, 0.5 mmol) were used. The yield is 316 mg (74%). Crystals for X-ray diffraction were grown by diffusion of hexane to a concentrated solution of $(NBu_4)_2[Fe(tcdt)_2]_2$ in dichloromethane. Elemental analyses Calcd: C, 39.37; H, 4.25; N, 1.63; Found: C, 40.39; H, 4.29; N, 1.57.

DOI: 10.1021/jacs.6b05040
J. Am. Chem. Soc. 2016, 138, 11654−11663

X-ray Crystallography. Crystals were placed onto the tips of glass capillary tubes or fibers and mounted on a Bruker SMART CCD platform diffractometer for data collection. For each crystal a preliminary set of cell constants and an orientation matrix were calculated from reflections harvested from three orthogonal wedges of reciprocal space. Full data collections were carried out using Mo Kα radiation (0.71073 Å, graphite monochromator) with frame times ranging from 25 to 60 s and at a detector distance of approximately 4 cm. Randomly oriented regions of reciprocal space were surveyed: three to six major sections of frames were collected with 0.50° steps in ω at three to six different φ settings and a detector position of −38° in 2θ. The intensity data were corrected for absorption.[56] Final cell constants were calculated from the *xyz* centroids of about 4000 strong reflections from the actual data collections after integration.[57]

Structures were solved using SIR97[58] and refined using SHELXL-97.[59] Space groups were determined on the basis of systematic absences, intensity statistics, or both. Direct-methods solutions were calculated, which provided most non-hydrogen atoms from the *E* map. Full-matrix least-squares/difference Fourier cycles were performed which located the remaining non-hydrogen atoms. All non-hydrogen atoms were refined with anisotropic displacement parameters. All hydrogen atoms were placed in ideal positions and refined as riding atoms with relative isotropic displacement parameters. Full-matrix least-squares refinements on F^2 were run to convergence.

Mössbauer Spectroscopy. All solid samples for ^{57}Fe Mössbauer spectroscopy were run on nonenriched samples of the as-isolated complexes. Each sample was prepared under ambient conditions and loaded into a Delrin Mössbauer sample cup for measurements. Low temperature ^{57}Fe Mössbauer measurements were performed using a See Co. MS4Mössbauer spectrometer integrated with a Janis SVT-400T He/N_2 cryostat for measurements at 80 K. Isomer shifts were determined relative to α-Fe at 298 K. All Mössbauer spectra were fit using the program WMoss (SeeCo).[60]

Hydrogen Evolution Studies. Photocatalytic hydrogen evolution experiments were performed in a custom-built 16-well apparatus. Samples in EtOH/H_2O (1/1) containing varying amounts of Fe dithiolene catalysts, water-soluble CdSe QDs with different capping agents and ascorbic acid (AA) sacrificial electron donors were prepared in 40 mL scintillation vials and protected from light before use. Total volume of the solution in each sample was 5 mL, the pH of the reaction solution was adjusted to 4.5 by the addition of NaOH or HCl. Control experiments were carried out under similar conditions in the absence of each component (e.g., CdSe QDs, AA, or catalysts). The samples were placed into a temperature-controlled block at 15 °C and sealed with an airtight cap fitted with a pressure transducer and a rubber septum. The samples were then purged with a mixture of gas containing 4:1 N_2/CH_4 with methane serving as an internal reference for GC analysis at the end of the experiment. The samples were irradiated from below the vials with high-power Philips LumiLED Luxeon Star Hex green (520 nm) 700-mA LEDs. The light power of each LED was set to 150 mW and measured with an L30 A Thermal sensor and a Nova II power meter (Ophir-Spiricon). The samples were swirled using an orbital shaker at 110 rpm. The pressure changes in the vials were recorded using a Labview program from a Freescale semiconductor sensor (MPX4259A series). At the end of the experiment, the headspace of the vials was characterized by gas chromatography to ensure that the measured pressure change was a consequence of hydrogen generation and to confirm that the amount of hydrogen calculated by the change in pressure corresponded to the amount determined by GC analysis. The amounts of hydrogen evolved were determined using a Shimadzu GC-17A gas chromatograph with a 5-Å molecular sieve column (30 m, 0.53 mm) and a thermal conductivity detector, and were quantified by a calibration plot relative to the internal CH_4 standard.

Systems with Ascorbic Acid Sacrificial Donors. The net reaction for photochemical hydrogen generation using ascorbic acid as the sacrificial donor can be expressed by the following equation in which H_2A is ascorbic acid and A is dehydroascorbic acid:

$$H_2A \xrightarrow{h\nu} A + H_2$$

The formation of A and H_2 from ascorbic acid has been determined to be thermodynamically unfavorable by 0.41 V at pH 4.[8]

RESULTS AND DISCUSSION

Synthesis and Structural Studies. Complexes **1**−**4** were synthesized by reacting the iron precursor ($Fe(NO_3)_3{\cdot}9H_2O$) with the corresponding dithiolate ligands in methanol under an N_2 atmosphere. For the synthesis of complex **4**, the 3,4,5,6-tetrachlorobenzene-1,2-dithiol ligand was prepared separately as described in the Experimental Section. All four complexes were isolated as anions with tetrabutylammonium as the countercation in relatively high yield (65−74%) and they are stable in the solid state under ambient conditions. Their molecular structures are shown in Scheme 1. The purities of complexes **1**−**4** have been confirmed by elemental analyses which match well with theoretically calculated values (see Experimental Section).

Scheme 1. Molecular Structures of Various Fe-Dithiolene Catalysts

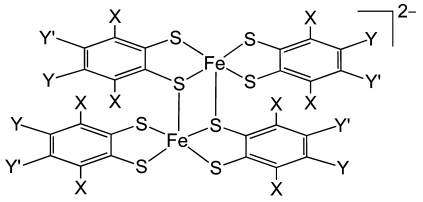

1	$[Fe(bdt)_2]_2^{2-}$	X = Y = Y' = H
2	$[Fe(tdt)_2]_2^{2-}$	X = Y = H; Y' = CH_3
3	$[Fe(dcbdt)_2]_2^{2-}$	X = Cl; Y = Y' = H
4	$[Fe(tcbdt)_2]_2^{2-}$	X = Y = Y' = Cl

The solid-state molecular structures of complexes **1**−**4** were determined by single-crystal X-ray diffraction (see Figure 1). The detailed crystallographical information is listed in Tables S1−S4. As shown in Figure 1, all four formally Fe(III) bis dithiolene complexes exist as dianionic dimers and exhibit similar structural characteristics. The Fe_2S_2 rhombus in each dimer is located on a crystallographic center of symmetry with each iron center having a tetragonal-pyramidal coordination geometry. Two dithiolate ligands occupy the basal sites, while the axial site contains a bridging dithiolate S ligand that serves as a basal ligand for the centrosymmetrically related Fe atom in the dimer. For all four complexes, the axial Fe−S bonds holding the two Fe-$(dithiolene)_2^-$ moieties together are longer than the basal Fe−S bonds *within* the chelate rings (Table 1).[44,61−63] The structural results are thus entirely consistent with the notion previously that in solution the dimers exist in equilibrium with the corresponding monomers.[62] Additionally, the S−Fe−S′ bond angle in each Fe_2S_2 rhombus increases in going from complexes **1** and **2** to complexes **3** and **4**, suggesting greater steric strain in the latter caused by the chloride substituents. Another feature of the structure of **1** that is recognized in the Mössbauer spectrum of the sample discussed below is that **1** crystallizes in the triclinic space group P1-bar with *two* crystallographically independent half-dimers in the asymmetric unit. The two dimers are structurally similar except for the Fe···Fe separations which are very significantly different (3.2066(6) Å in **1a** and 3.0398(6) Å in **1b**). In the other structures as well, the Fe···Fe separations exhibit a significant variance being 3.2126(14), 2.9623(7) and 3.0424(11) Å in **2**, **3** and **4**, respectively.

Spectroscopic Characterization and Redox Chemistry of Fe-Dithiolene Complexes. The UV−vis absorption spectra

DOI: 10.1021/jacs.6b05040
J. Am. Chem. Soc. 2016, 138, 11654−11663

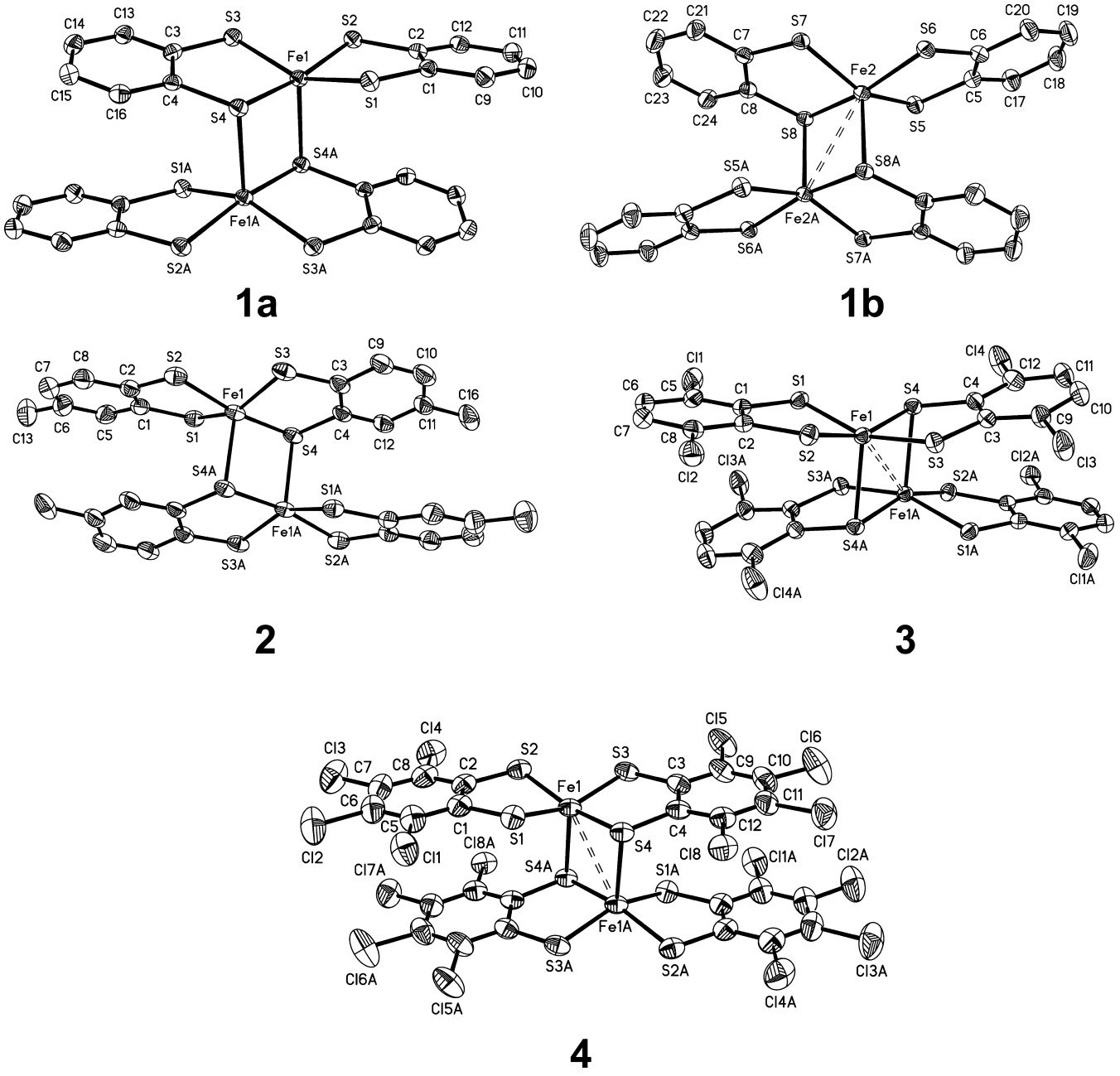

Figure 1. Structures of complexes **1**−**4**. Complex **1** has two crystallographically independent dimeric dianions which are shown separately as **1a** and **1b.** Dashed lines between Fe atoms indicate distances shorter than 3.05 Å. The counter cations (NBu_4^+) are omitted for simplicity.

of complexes **1**−**4** were determined in acetonitrile at room temperature. Complexes **1**−**4** all show intense high-energy bands in the UV region, corresponding to spin-allowed intraligand (π−π^*) transitions.[24] As shown in Figure 2, all four complexes exhibit broad low-energy bands in the 450−650 nm region, which can be described as charge transfer transitions based on their relative intensities.[45,64] The absorption envelopes of the charge transfer bands indicate at least three transitions for each complex in the 450−650 nm region. The two highest energy bands for **1**−**3** are similar in value, but differ in relative intensity (**1**: 490, 520 nm; **2**: 490, 525 nm; **3**: 492, 522 nm), whereas for complex **4** the observed highest energy transition is red-shifted to 522 nm with a shoulder at 562 nm. In view of the existence of multiple charge transfer transitions for each of the complexes, and the fact that they exist in monomer−dimer equilibria in fluid solution, attention turned to other methods of definitive characterization of **1**−**4**.

Mössbauer measurements on solid samples of complexes **1**−**4** were performed at 80 K (see details in Experimental Section). The spectra of all four complexes are clean with insignificant impurity peaks, as shown in Figure 3. Complexes **2**−**4** exhibit only a single quadrupole doublet, whereas complex **1** shows two quadrupole doublets in an approximate ratio of 1:1. The latter observation is attributed to the two crystallographically *independent* dinuclear dianions in the asymmetric unit as determined by X-ray diffraction (Table 1, Figure S1). For **1**, the two independent dianions have significantly different Fe···Fe separations and therefore exhibit slightly different quadrupole splitting parameters (δ = 0.34 mm/s, ΔE_Q = 2.62 mm/s vs δ = 0.34 mm/s, ΔE_Q = 3.05 mm/s). Complexes **2**−**4** possess similar

DOI: 10.1021/jacs.6b05040
J. Am. Chem. Soc. 2016, 138, 11654−11663

Table 1. Key Bond Distances and Angles in Complexes 1−4

	bond distances (Å)				
	complex **1**		complex **2**	complex **3**	complex **4**
Fe(1)−S(1)	2.2350(6)	2.2301(6)	2.2315(14)	2.2207(7)	2.2167(12)
Fe(1)−S(2)	2.2250(6)	2.2242(6)	2.2155(16)	2.2209(7)	2.2125(12)
Fe(1)−S(3)	2.2289(6)	2.2348(6)	2.2241(15)	2.2323(7)	2.2280(12)
Fe(1)−S(4)	2.2365(6)	2.2317(6)	2.2312(15)	2.2292(7)	2.2172(11)
Fe(1)−S(4)#1	2.4945(6)	2.4247(6)	2.4813(13)	2.4461(7)	2.4808(11)
S(4)−Fe(1)#1	2.4945(6)	2.4247(6)	2.4812(13)	2.4462(7)	2.4807(11)
Fe(1)−Fe(1)#1	3.2066(6)	3.0398(6)	3.2126(14)	2.9623(7)	3.0424(11)
	bond angles (deg)				
	complex **1**		complex **2**	complex **3**	complex **4**
S(2)−Fe(1)−S(1)	88.84(2)	89.29(2)	88.68(6)	88.68(3)	89.00(5)
S(3)−Fe(1)−S(4)	89.65(2)	88.93(2)	88.86(6)	89.43(3)	89.92(4)
S(4)−Fe(1)−S(4)#1	94.84(2)	98.61(2)	94.21(5)	101.52(2)	99.49(4)
Fe(1)−S(4)−Fe(1)#1	85.15(2)	81.39(2)	85.78(5)	78.48(2)	80.51(4)

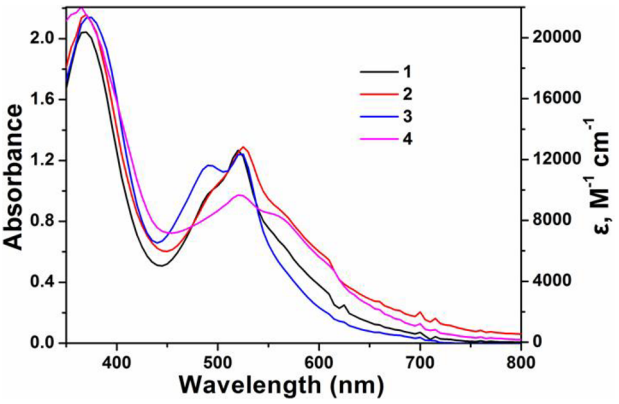

Figure 2. UV−vis absorption spectra of 0.1 mM complexes **1**−**4** in acetonitrile.

Mössbauer parameters to those of **1** (**2**: δ = 0.32 mm/s, ΔE_Q = 2.91 mm/s; **3**: δ = 0.32 mm/s, ΔE_Q = 2.82 mm/s; **4**: δ = 0.32 mm/s, ΔE_Q = 3.02 mm/s). These results are in agreement with data in the literature[44,62,63] on these and similar Fe dithiolene dimeric compounds. Three of these complexes (**1**, **2**, **4**) have previously been reported to have intermediate spin ferric ion (S_{Fe} = 3/2). Since there are two identical Fe ions (S_{Fe} = 3/2) in each dinuclear dianion complex, it is important to understand the total spin state per dianion. Previous temperature-dependent magnetic studies on solid-state samples were consistent with the presence of intramolecular antiferromagnetic coupling between the S_{Fe} = 3/2 ferric ions in each dianion, resulting in an S = 0 diamagnetic ground state.[44,63,65]

In light of dimer dissociation into monomers in fluid solution, the ^{1}H NMR spectra of complexes **1**−**4** in deuterated tetrahydrofuran (THF-d_8) were examined. The complexes were found to exhibit broad proton resonance signals, supporting the notion of dissociation into paramagnetic monoanions in solution. Magnetic susceptibility measurements for complexes **1**−**4** in solution were carried out using the Evans method.[54] The experimentally calculated effective magnetic moments for complexes **1** and **2** are both 5.01 μ_B, consistent with four unpaired electrons per dianion, whereas for complexes **3** and **4**, two sets of effective magnetic moment values are obtained (**3**: μ_{eff} = 4.90 μ_B and 6.01 μ_B; **4**: μ_{eff} = 5.03 μ_B and 5.82 μ_B). Since these

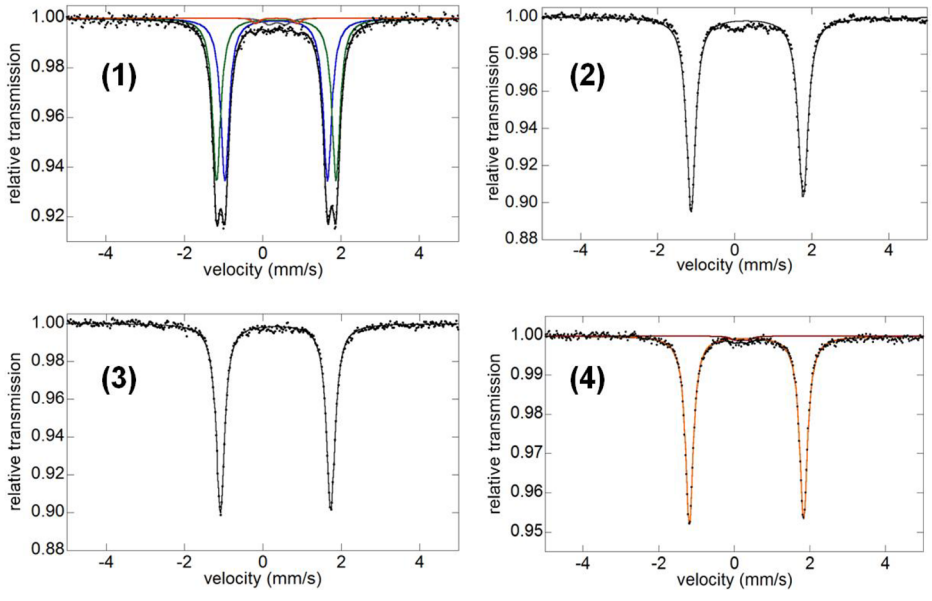

Figure 3. 80 K Mössbauer spectra of solid complexes **1**−**4**.

DOI: 10.1021/jacs.6b05040
J. Am. Chem. Soc. 2016, 138, 11654−11663

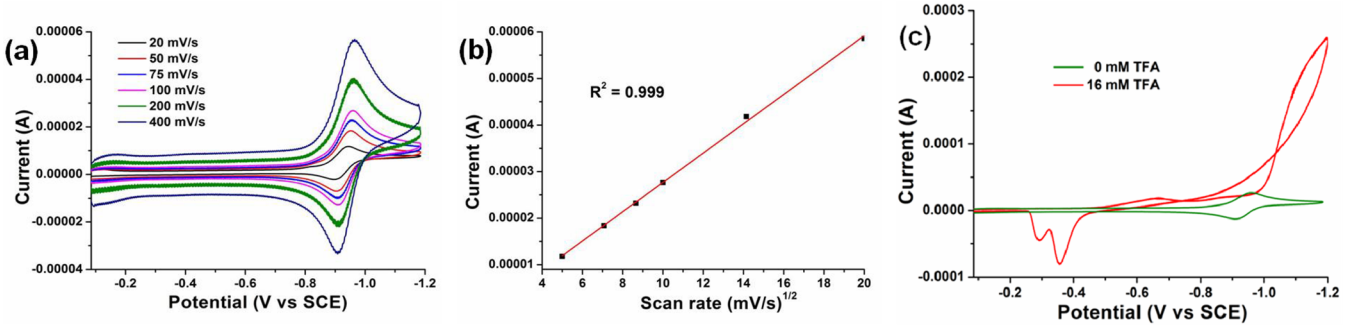

Figure 4. (a) Cyclic voltammograms of 0.5 mM complex **2** at different scan rates in the range of 0 to −1.2 V; (b) the plot of maximum peak currents versus the square root of scan rates; and (c) cyclic voltammograms of 0.5 mM complex **2** with varying concentrations of trifluoroacetic acid. Conditions: 0.5 mM complex **2**, 0.1 M $TBAPF_6$ electrolyte in acetonitrile, 1 M H_2O, glassy carbon working electrode, Pt auxiliary electrode, SCE reference electrode.

results were obtained at a particular temperature and a single concentration, they simply serve as a characterization of the specific samples employed. The notion of a dimer−monomer equilibrium is important in the solution chemistry of these complexes[61,62] and may well play a role in the catalytic behavior discussed below.

Cyclic voltammetric experiments were conducted in acetonitrile media for complexes **1**−**4** at room temperature under an Ar atmosphere. Figure 4 shows the representative CV curves of 0.25 mM complex **2** at different scan rates. A reversible reduction peak at −0.928 V vs SCE was observed, corresponding to the $[FeL_2]_2^{2-}/[FeL_2]_2^{3-}$ couple. Table S5 summarizes the first reversible reduction potentials of all four Fe dithiolene complexes, which range from −0.723 V to −0.928 V vs SCE, depending on the electron donating ability of the dithiolene ligand. A plot of peak current vs $(\text{scan rate})^{1/2}$ for **2** exhibits a linear dependence (R^2 = 0.999, Figure 4b), consistent with a diffusion-controlled interfacial redox process. To examine the potential activity of these complexes for proton reduction, aliquots of trifluoroacetic acid were added to solutions of the complexes in deaerated CH_3CN containing 1 M H_2O. As shown in Figure 4c for complex **2**, addition of trifluoroacetic acid triggers significant current enhancement near the onset of the reversible redox couple, indicating that the reduced form of complex **2** is active for proton reduction. Similar behaviors were also observed for complexes **1**, **3**, and **4** (Figure S5), where the current enhancement was triggered by addition of trifluoroacetic acid. Interestingly, under otherwise identical experimental conditions, complex **2** exhibits highest catalytic current enhancement followed in order by **1**, **4** and **3**. These results reveal the inherent differences of the four complexes toward catalytic proton reduction.

Photocatalytic H_2 Evolution Activity. Photocatalytic experiments for hydrogen evolution were performed using water-soluble CdSe QDs as the photosensitizer, ascorbic acid (AA) as the sacrificial electron donor, and complexes **1**−**4** as water reduction catalysts in deaerated EtOH/H_2O (1/1 v/v) solvent. The amount of H_2 produced was monitored in real time using a pressure transducer on each sample and quantified by GC analysis of the headspace gas at the end of the irradiation period (see Experimental Section). While AA is employed solely as an electron source in these studies, we note that the net conversion of AA to dehydroascorbic acid + H_2 is actually energy storing by approximately 20 kcal/mol.[8,16] The water-soluble CdSe QDs used for the photochemical experiments were prepared through ligand exchange of CdSe-TOPO QDs with the corresponding water-solubilizing capping agent (DHLA, S3, MPA, and MUA shown below with thiolates coordinating to surface-bound Cd^{2+} and carboxylic acid groups significantly deprotonated at pH 4.5). UV−vis Spectra of the CdSe QDs were recorded before and after ligand exchange and are shown in Figure S6.

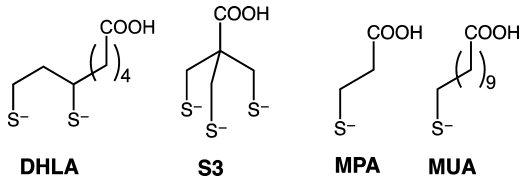

Although appropriate reaction time for ligand exchange does not affect the size of CdSe QDs (Figure S6), longer reaction time or the addition of large excesses of water-solubilizing capping agents can result in a decrease of QD size. The size of CdSe QDs prepared for H_2-generating experiments is in the range of 2.5−2.7 nm, corresponding to their first excitonic peaks in the range of 515−530 nm. CdSe QDs of this size have a conduction band (CB) edge as negative as −1 V vs NHE,[66] making photogenerated electrons sufficiently negative to reduce complexes **1**−**4** (Table S5).

In initial catalytic studies involving complexes **1**−**4**, CdSe-DHLA QDs were employed with 520 nm LED light leading to the hydrogen evolution profiles depicted in Figure 5. Under minimally optimized conditions, the turnover numbers (TONs) per Fe atom after 80 h of irradiation reached 20 600, 29 400,

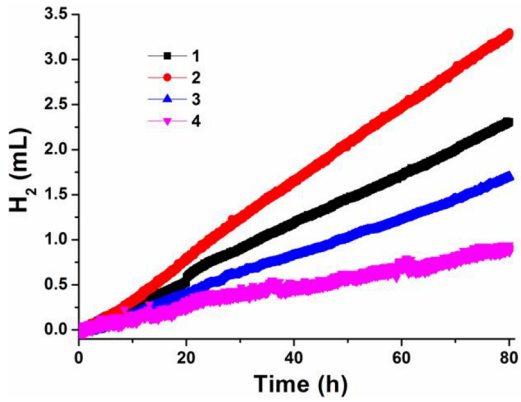

Figure 5. Photocatalytic hydrogen production from systems containing Fe-dithiolene complexes (0.5 μM), CdSe-DHLA QDs (525 nm, 2 μM), AA (0.2 M) in 5 mL EtOH/H_2O (1/1) at pH = 4.5 upon irradiation with 520 nm LED at 15 °C and 1 atm initial pressure of N_2/CH_4 (4/1) with CH_4 as an internal standard for H_2 quantification by GC analysis.

DOI: 10.1021/jacs.6b05040
J. Am. Chem. Soc. 2016, 138, 11654−11663

15 200, and 8000 for catalysts **1**−**4**, respectively, with complex **2** showing highest activity. In view of the fact that earlier studies had shown that the DHLA capping agents on the CdSe QDs are labile and dissociate into the solution even in the absence of light irradiation,[22] examination of the interaction of DHLA with catalyst complexes **1**−**4** was examined by UV−vis spectroscopy, the results of which are shown in Figure S7. For complexes **1** and **2**, the benzenedithiolate ligands L are readily displaced by DHLA, resulting in a pale yellow solution, indicative of the formation of new species such as $[Fe(L)_x(DHLA)_y]^{n-}$ with $x = 0$ or 1. In contrast, substitution of the benzenedithiolate ligands L by DHLA is much slower for complexes **3** and **4**, although complete substitution is observed after 24 h at room temperature. The differences in the observed rates of substitution (Figure S7) may relate to the tendency of the $[Fe_2(dithiolene)_4]^{2-}$ anions to dissociate into monomeric $[Fe(dithiolene)_2]^{-}$ species even *without* reduction. The Co analogues of **1** and **2** exist as monomers in solution, whereas those of **3** and **4** exist in dimeric form. The rate of ligand replacement by DHLA also depends on its concentration (Figure S8), with a faster disappearance of the characteristic absorption band of **2** with increased concentrations of DHLA, supporting the formation of DHLA-containing species. In light of the DHLA/dithiolene ligand exchange reactions occurring, the H_2-generating activity observed in Figure 5 does *not* accurately reflect the *catalytic* activity of complexes **1**−**4** due to formation of $[Fe(L)_x(DHLA)_y]^{n-}$ species during H_2 formation.

The exchange inertness of the S3 capping agent from the surface of CdSe QDs has previously been described in studies involving Ni DHLA and Co dithiolene catalysts.[32] Experiments were therefore undertaken with CdSe-S3 light absorbers and complexes **1**−**4**, as well as with $Fe(NO_3)_3$ as a catalyst precursor, to determine catalyst activity in the absence of DHLA substitution. Figure 6 illustrates the photocatalytic hydrogen evolution profiles for complexes **1**−**4** using CdSe-S3 QDs as the photosensitizer. The overall activity of the four complexes is lower than that of the systems using CdSe-DHLA light-absorbers. In terms of TONs for these CdSe-S3 systems after 80 h irradiation, the activity order is **2** > **1** > **3** > **4** with TONs of 17 600, 11 100, 9100, and 8400, respectively. In control experiments, removal of any component in the WRC system (catalyst **1**−**4**, AA or CdSe-S3 QDs) or running the catalysis in dark generated little or no H_2 (Chart S1) The observed order of activity for complexes **1**−**4** was found to correlate with the reduction potential for the $[FeL_2]_2^{2-/3-}$ couple (−0.928, −0.898, −0.764, −0.723 V vs SCE), and was thus similar to the order of activity reported for CdSe-S3 systems having the analogous Co bis dithiolene catalysts.[32] The observed order of activity for complexes **1**−**4** under photochemical conditions is consistent with their electrocatalytic proton reduction activity as shown in Figure 6 and Figure S5. Finally, for the system $Fe(NO_3)_3$/CdSe-S3/AA in which no dithiolene ligands are present, irradiation after 80 h gave insignificant amount of H_2.

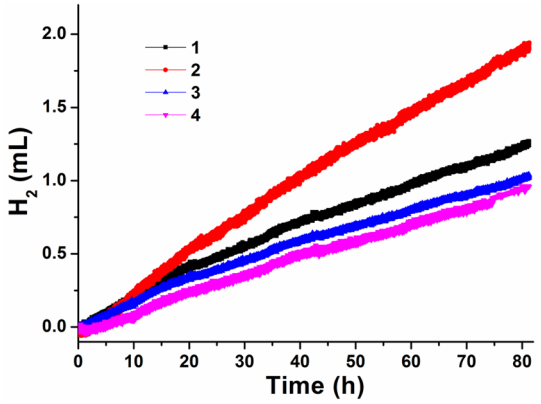

Figure 6. Photocatalytic hydrogen production from systems containing Fe-dithiolene complexes (0.5 μM), CdSe-S3 QDs (520 nm, 2 μM), AA (0.2 M) in 5 mL EtOH/H_2O (1/1) at pH = 4.5 upon irradiation with 520 nm LED at 15 °C and 1 atm initial pressure of N_2/CH_4 (4/1) with CH_4 as an internal standard for H_2 quantification by GC analysis.

Changes in relative amounts of components in the systems **1**−**4**/CdSe-S3/AA yielded additional insight. A 8-fold greater concentration of **2** in the reaction solution led to a corresponding increase of evolved H_2, with the amount increasing from ∼1.28 mL (57 μmol) to 2.78 mL (124 μmol) (Figure S9) although the TON decreased from ∼22 800 to ∼6200, suggesting that at the higher concentration, the catalyst is no longer the limiting component. The concentrations of CdSe-S3 QDs and the sacrificial electron donor (AA) also affect the rates and yields of H_2 production. An increase in the concentration of CdSe-S3 QDs from 1 μM to 4 μM results in growth of H_2 yields from ∼1.29 mL (58 μmol) to 2.80 mL (125 μmol) corresponding to a change in TON from ∼11 500 to 25 000 (Figure S10). Whereas an increase in AA concentration also impacts positively H_2 evolution, at concentrations greater than 0.4 M, saturation may be approached (Figure S11).

The addition of DHLA to the S3-containing systems ($Fe(NO_3)_3$/CdSe-S3/AA), results in significant increases in H_2-generating capability. For the $Fe(NO_3)_3$-containing system, the addition of 80 equiv of DHLA gave great enhancement of H_2 evolution in terms of both rate and yield (the TON reaches ∼15 300 in the presence of DHLA, compared to ∼3900 in the absence of DHLA), indicating catalytic activity results from an in situ-formed Fe DHLA complex (Figure S12). For the system containing the Fe dithiolene complexes **1**−**4** and CdSe-S3/AA, 160 equiv of DHLA were added, and the systems were allowed to age for 2 h prior to irradiation to permit simple ligand exchange. The H_2 production profiles for the four systems are *similar* to each other (Figure S13), as well as to that of the $Fe(NO_3)_3$/CdSe-S3/AA system (Figure S14). These results thus support the notion of a *common* Fe DHLA catalyst produced in each system.

The addition of *smaller* amounts of DHLA to the **2**/CdSe-S3/AA system, however, indicate the formation of a mixed ligand catalyst. The results are summarized in Table S6. Specifically, the addition of 1 or 2 equiv of DHLA relative to catalyst yields an *increase* in H_2 yields, but for further additions of 4−80 equiv DHLA, the rate declines slightly and levels off to a value slightly lower than that observed for the system $Fe(NO_3)_3$/CdSe-S3/AA + 80 equiv DHLA. The results thus indicate that for the most active system in which the iron dithiolene complex **2** and DHLA exist, the in situ-generated catalyst contains both DHLA and dithiolene ligands for H_2 production.

Long-Term Stability and Reusability Evaluation. Several experiments were conducted to assess long-term system robustness and reusability of system components. Whereas the rate and yield of H_2 generation exhibited a stable profile in initial catalytic runs over >80 h of irradiation (Figure 7), reuse of the system from the initial run led to decreases in both rate and yield of H_2 production. The decline in system activity is attributed (a) depletion of AA, (b) instability of catalyst **2**, and (c) change in pH of the reaction solution. With regard to (c), system pH following

DOI: 10.1021/jacs.6b05040
J. Am. Chem. Soc. 2016, 138, 11654−11663

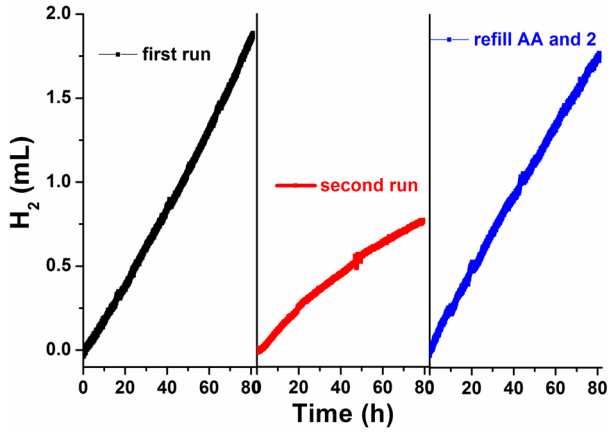

Figure 7. Photocatalytic hydrogen production from systems containing complex **2** (0.5 μM), CdSe-S3 QDs (523 nm, 2 μM), AA (0.2 M) in 5 mL EtOH/H_2O (1/1) at pH = 4.5 upon irradiation with 520 nm LED at 15 °C and 1 atm initial pressure of N_2/CH_4 (4/1): (a) black curve: initial run of the catalytic solution; (b) red curve: second run of the reaction solution; and (c) blue line: the reaction solution following (b) to which 0.5 μM complex **2** and 1 mL 1 M AA stock solution were added.

a second period of irradiation was found to increase to 5.6, consistent with proton removal from the system to form H_2 and the declining capacity of the ascorbic acid/ascorbate buffer. The addition of 1 mL of 1 M AA and 25 μL of 0.1 mM solution of catalyst **2** to a previously irradiated system yielded a rate and yield of H_2 production during a *third* period of irradiation that were almost the same as those of the initial run, as shown in Figure 7. To assay further the robustness of the photosensitizers, previously employed CdSe QDs were isolated from reaction solutions by centrifugation and then redispersed in slightly basic water for subsequent catalytic experiments. The redispersed CdSe-S3 QDs solution is quite clear, while that of CdSe-DHLA QDs appears slightly cloudy (possibly as a consequence of DHLA ligand dissociation resulting in lower capping agent coverage). The UV−vis spectra of solutions of isolated CdSe-S3 QDs and CdSe-DHLA QDs have similar absorption profiles, both to each other and to ones obtained from the original QDs solutions, respectively (Figure S15). Light-driven H_2 evolution experiments using either isolated CdSe-DHLA QDs or CdSe-S3 QDs plus fresh catalyst and AA solution give similar H_2 generation rates and yields to those obtained from systems using fresh CdSe QDs (Figure S16 and Figure S17), indicating the relative stability of the QD light absorbers during the examined periods of irradiation.

Effect of Surface Ligand Coverage of CdSe QDs on H_2 Generation Activity. From studies above, it is evident that both the nature and amount of capping agent affect system activity, in accord with studies on the redox chemistry involving semiconductor nanoparticles.[67] To probe this notion further, several experiments were conducted. In one study, CdSe-S3 and CdSe-DHLA QDs with varying amounts of water-solubilizing capping agents were prepared and characterized and the amounts of capping agent on the CdSe QD surface were quantified by ^{1}H NMR spectroscopy. Specifically, the S3 and DHLA capping agents were removed from the QD surface by addition of 6 M HCl to pH 0, thus causing precipitation of the CdSe particles.[68] The dissociated capping agents were separated from the quantum dots, redissolved in DMSO-d_6 and then quantified by ^{1}H NMR spectroscopy using benzene as an internal standard (see Experimental details in the SI). The molar ratio of DHLA or S3 to CdSe QDs was used to denote different CdSe QDs light-absorbers, for example, 100 S3 units per CdSe dot indicates the ratio of S3 capping agents per CdSe dot is 100.

Figure 8 illustrates results of the photogeneration of hydrogen using CdSe-S3 QDs photosensitizers that had been reacted with

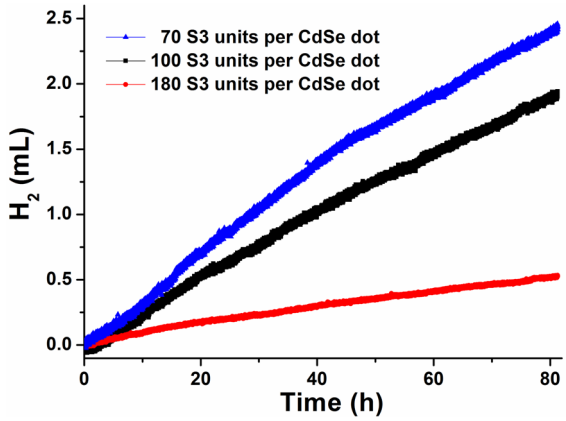

Figure 8. Photocatalytic hydrogen production from systems containing complex **2** (0.5 μM), 2 μM CdSe-S3 QDs (blue curve: 523 nm with 70 S3 units; black curve: 525 nm with 100 S3 units; red curve: 515 nm with 180 S3 units), AA (0.2 M) in 5 mL EtOH/H_2O (1/1) at pH = 4.5. Irradiation with 520 nm LED at 15 °C and 1 atm initial pressure of N_2/CH_4 (4/1) with CH_4 as a GC analysis internal standard for H_2 quantification.

different amounts of S3 capping agent prior to irradiation and the TONs obtained for light-driven hydrogen generating experiments are summarized in Table S7. The results show that decreasing the amount of S3 capping agents on CdSe from 180 to 100 to 70 units per CdSe dot *increases* the rate and final yield of H_2 generation (the TONs increase from 4600 to 17 600 to 20 700, respectively, for complex **2**-catalyzed reactions). Similarly, for catalytic systems containing DHLA-capped CdSe QDs with complex **2** as the catalyst and AA, an increase in activity is noted with a decrease in DHLA units per CdSe QD from 210 to 140 (Figure S18, Table S8); however, the difference between the obtained TONs is much smaller than for the systems using S3-capped CdSe QDs. The reduced magnitude of the effect with DHLA capping agents relative to S3 is consistent with the lability of DHLA for dissociation from the CdSe QD surface in contrast with the inertness of the S3 capping agent.

In addition to the results on the variation of capping agent amounts for CdSe-S3 and CdSe-DHLA catalytic systems, it was also found that photogeneration of H_2 using CdSe QDs with the capping agents mercaptopropionoic acid (MPA) and mercaptoundecanoic acid (MUA) exhibit different behaviors in activity. Figure 9 shows hydrogen evolution data using CdSe-MPA, complex **2** as catalyst and AA as electron donor. In the absence of external DHLA, ~2.4 mL (107 μmol) hydrogen gas was produced after 120 h irradiation, corresponding to a TON of ~21 300. Interestingly, addition of 80 equiv of DHLA to the catalytic solution dramatically enhances the rate and yield of H_2 generation with 12.4 mL (553 μmol) H_2 generated (5 times that of the system without DHLA), consistent with a TON of 110 600. Very recently, Wu and co-workers reported a related photochemical hydrogen evolution system using CdSe-MPA QDs as photosensitizer, an Fe_2S_2 hydrogenase mimic bound to poly(acrylic acid) (PPA-*g*-Fe_2S_2) as the catalyst and AA as the electron donor at pH 4.0.[40a] A blue LED at 450 nm was

DOI: 10.1021/jacs.6b05040
J. Am. Chem. Soc. 2016, 138, 11654−11663

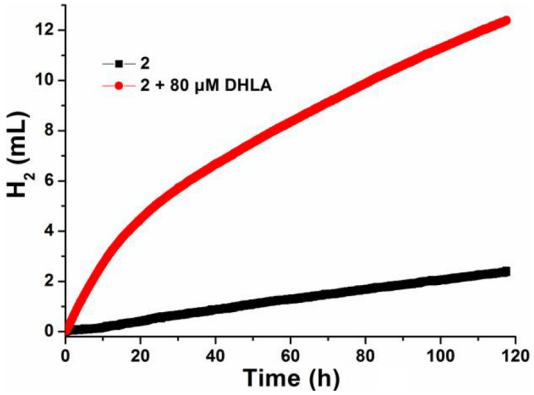

Figure 9. Photocatalytic hydrogen production from systems containing CdSe-MPA QDs (518 nm, 1 μM), complex **2** (0.5 μM; black curve) or complex **2** (0.5 μM) + DHLA (80 μM) (red curve), AA (0.2 M) in 5 mL EtOH/H_2O (1/1) at pH = 4.5 upon irradiation with 520 nm LED at 15 °C and 1 atm initial pressure of N_2/CH_4.

employed for irradiation in those systems. Under optimal conditions, a TON of ~27 100 was obtained after 8 h irradiation, but the system tended to stop working upon prolonged irradiation. While the relative activity and final TONs obtained in their systems are comparable to those reported in current work, the results cannot be compared directly due to many differences between them and the present results with respect to experimental conditions and analyses.

The system with MUA as the surface capping agent is less active than the corresponding MPA system, but like the MPA system, it exhibits an increase in activity upon the addition of DHLA (Figure S19). In either case (with CdSe-MUA only or with CdSe-MUA + DHLA), hydrogen evolution results are lower (TONs of 11 400 without DHLA and 29 200 with 160 equiv DHLA) than those obtained with the corresponding MPA systems. It can be conjectured that the longer aliphatic chains of MUA relative to MPA inhibit electron transfer to the catalyst needed for hydrogen generation.

All of the results for photochemical hydrogen formation from protons for the systems described here illustrate the importance of surface capping agents and their dynamics in determining their relative catalytic activity. It appears that for photochemical H_2 production, surface capping agents may influence both exciton lifetime in CdSe QDs upon irradiation and electron transfer rates within the system for such H_2-generating catalysis.[67,69] More detailed studies to better understand the mechanism on how capping agents affect catalytic activity are in progress.

CONCLUSIONS

In this study, four closely related Fe bis(benzenedithiolate) complexes have been synthesized, characterized and studied as catalysts for the light-driven generation of H_2. All four formally Fe(III) bis dithiolene complexes are isolated as dianionic dimers with similar structural characteristics in the solid state, although significant differences in nonbonding Fe···Fe separations are noted. Cyclic voltammetric experiments in the presence of trifluoroacetic acid reveal that the reduced monomeric forms of the complexes—that is, $[Fe(\text{dithiolate ligand})_2]^{2-}$—are active for proton reduction. When used with water-solubilized CdSe QDs as the light absorber and ascorbic acid as the sacrificial electron donor, all four complexes exhibit catalytic hydrogen-evolving activity under visible light irradiation (520 nm). The complex with the most electron-donating dithiolene ligand exhibits the highest activity when using different types of CdSe light-absorbers (CdSe-DHLA, CdSe-S3, CdSe-MPA, and CdSe-MUA). The overall order of activity correlates with the reduction potential of the formally Fe(III) dimeric dianions.

The catalytic activity of these complexes is found to depend on the nature of the water-solubilizing capping agent for the CdSe light absorbers. When S3, which has been established to be inert to substitution, is employed, modest activities are found that correlate with the reduction potential of the dimeric bis-(dithiolene) formally Fe(III) complexes. Upon addition of ≥80 equiv of DHLA, catalytic activity increases greatly and shows similar levels of activity for all four bis dithiolene complexes, as well as for $Fe(NO_3)_3$ as an Fe(III) source, indicative of a common in situ-formed $Fe(DHLA)_x$ catalyst. For the additions of 1−4 equiv of DHLA to the CdSe-S3 system, the catalytic activity is consistent with the formation of a mixed Fe-$(DHLA)_x(\text{dithiolene})_y^{z-}$ that is most active for the toluenedithiolate system.

ASSOCIATED CONTENT

Supporting Information

The Supporting Information is available free of charge on the ACS Publications website at DOI: 10.1021/jacs.6b05040.

Detailed experimental procedures for water-soluble ligand exchange, X-ray crystallographic data, UV−vis spectra, electrochemistry data, and additional photocatalytic hydrogen production data (PDF)

Crystal data (CIF)

AUTHOR INFORMATION

Corresponding Author

*eisenberg@chem.rochester.edu

Notes

The authors declare no competing financial interest.

ACKNOWLEDGMENTS

This research was supported by the Division of Chemical Sciences, Geosciences, and Biosciences, Office of Basic Energy Sciences, U.S. Department of Energy, Grant DE-FG02-09ER16121 for all syntheses, characterizations and H_2 generation studies. Mössbauer measurements were conducted with the support of National Science Foundation Grant CHE-1454370 to M. L. N. The receipt of an Alfred P. Sloan Fellowship to M. L. N. is gratefully acknowledged.

REFERENCES

(1) Graetzel, M. *Acc. Chem. Res.* **1981**, *14*, 376.
(2) Lewis, N. S.; Nocera, D. G. *Proc. Natl. Acad. Sci. U. S. A.* **2006**, *103*, 15729.
(3) Gray, H. B. *Nat. Chem.* **2009**, *1*, 7.
(4) Eisenberg, R. *Science* **2009**, *324*, 44.
(5) Lv, H.; Geletii, Y. V.; Zhao, C.; Vickers, J. W.; Zhu, G.; Luo, Z.; Song, J.; Lian, T.; Musaev, D. G.; Hill, C. L. *Chem. Soc. Rev.* **2012**, *41*, 7572.
(6) Lehn, J. M.; Sauvage, J. P. *Nouv. J. Chim.* **1977**, *1*, 449.
(7) Kalyanasundaram, K.; Kiwi, J.; Grätzel, M. *Helv. Chim. Acta* **1978**, *61*, 2720.
(8) Brown, G. M.; Brunschwig, B. S.; Creutz, C.; Endicott, J. F.; Sutin, N. *J. Am. Chem. Soc.* **1979**, *101*, 1298.
(9) DeLaive, P. J.; Sullivan, B. P.; Meyer, T. J.; Whitten, D. G. *J. Am. Chem. Soc.* **1979**, *101*, 4007.
(10) Streich, D.; Astuti, Y.; Orlandi, M.; Schwartz, L.; Lomoth, R.; Hammarstroem, L.; Ott, S. *Chem. - Eur. J.* **2010**, *16*, 60.

DOI: 10.1021/jacs.6b05040
J. Am. Chem. Soc. 2016, 138, 11654−11663

(11) Li, X.; Wang, M.; Chen, L.; Wang, X.; Dong, J.; Sun, L. *ChemSusChem* **2012**, *5*, 913.
(12) Berggren, G.; Adamska, A.; Lambertz, C.; Simmons, T. R.; Esselborn, J.; Atta, M.; Gambarelli, S.; Mouesca, J. M.; Reijerse, E.; Lubitz, W.; Happe, T.; Artero, V.; Fontecave, M. *Nature* **2013**, *499*, 66.
(13) Artero, V.; Saveant, J.-M. *Energy Environ. Sci.* **2014**, *7*, 3808.
(14) Fihri, A.; Artero, V.; Razavet, M.; Baffert, C.; Leibl, W.; Fontecave, M. *Angew. Chem., Int. Ed.* **2008**, *47*, 564.
(15) Lazarides, T.; McCormick, T.; Du, P.; Luo, G.; Lindley, B.; Eisenberg, R. *J. Am. Chem. Soc.* **2009**, *131*, 9192.
(16) McNamara, W. R.; Han, Z.; Alperin, P. J.; Brennessel, W. W.; Holland, P. L.; Eisenberg, R. *J. Am. Chem. Soc.* **2011**, *133*, 15368.
(17) Zhang, P.; Jacques, P.-A.; Chavarot-Kerlidou, M.; Wang, M.; Sun, L.; Fontecave, M.; Artero, V. *Inorg. Chem.* **2012**, *51*, 2115.
(18) Singh, W. M.; Baine, T.; Kudo, S.; Tian, S.; Ma, X. A. N.; Zhou, H.; DeYonker, N. J.; Pham, T. C.; Bollinger, J. C.; Baker, D. L.; Yan, B.; Webster, C. E.; Zhao, X. *Angew. Chem., Int. Ed.* **2012**, *51*, 5941.
(19) Khnayzer, R. S.; Thoi, V. S.; Nippe, M.; King, A. E.; Jurss, J. W.; El Roz, K. A.; Long, J. R.; Chang, C. J.; Castellano, F. N. *Energy Environ. Sci.* **2014**, *7*, 1477.
(20) Helm, M. L.; Stewart, M. P.; Bullock, R. M.; DuBois, M. R.; DuBois, D. L. *Science* **2011**, *333*, 863.
(21) Small, Y. A.; DuBois, D. L.; Fujita, E.; Muckerman, J. T. *Energy Environ. Sci.* **2011**, *4*, 3008.
(22) Han, Z.; Qiu, F.; Eisenberg, R.; Holland, P. L.; Krauss, T. D. *Science* **2012**, *338*, 1321.
(23) Han, Z.; McNamara, W. R.; Eum, M.-S.; Holland, P. L.; Eisenberg, R. *Angew. Chem., Int. Ed.* **2012**, *51*, 1667.
(24) Han, Z.; Shen, L.; Brennessel, W. W.; Holland, P. L.; Eisenberg, R. *J. Am. Chem. Soc.* **2013**, *135*, 14659.
(25) Lv, H.; Guo, W.; Wu, K.; Chen, Z.; Bacsa, J.; Musaev, D. G.; Geletii, Y. V.; Lauinger, S. M.; Lian, T.; Hill, C. L. *J. Am. Chem. Soc.* **2014**, *136*, 14015.
(26) Lv, H.; Chi, Y.; van Leusen, J.; Kögerler, P.; Chen, Z.; Bacsa, J.; Geletii, Y. V.; Guo, W.; Lian, T.; Hill, C. L. *Chem. - Eur. J.* **2015**, *21*, 17363.
(27) Karunadasa, H. I.; Chang, C. J.; Long, J. R. *Nature* **2010**, *464*, 1329.
(28) Karunadasa, H. I.; Montalvo, E.; Sun, Y.; Majda, M.; Long, J. R.; Chang, C. J. *Science* **2012**, *335*, 698.
(29) Hawecker, J.; Lehn, J. M.; Ziessel, R. *Nouv. J. Chim.* **1983**, *7*, 271.
(30) Collin, J. P.; Sauvage, J. P. *Coord. Chem. Rev.* **1989**, *93*, 245.
(31) McCormick, T. M.; Han, Z.; Weinberg, D. J.; Brennessel, W. W.; Holland, P. L.; Eisenberg, R. *Inorg. Chem.* **2011**, *50*, 10660.
(32) Das, A.; Han, Z.; Haghighi, M. G.; Eisenberg, R. *Proc. Natl. Acad. Sci. U. S. A.* **2013**, *110*, 16716.
(33) Das, A.; Han, Z.; Brennessel, W. W.; Holland, P. L.; Eisenberg, R. *ACS Catal.* **2015**, *5*, 1397.
(34) Ruberu, T. P. A.; Dong, Y.; Das, A.; Eisenberg, R. *ACS Catal.* **2015**, *5*, 2255.
(35) Amirav, L.; Alivisatos, A. P. *J. Phys. Chem. Lett.* **2010**, *1*, 1051.
(36) Brown, K. A.; Dayal, S.; Ai, X.; Rumbles, G.; King, P. W. *J. Am. Chem. Soc.* **2010**, *132*, 9672.
(37) Brown, K. A.; Wilker, M. B.; Boehm, M.; Dukovic, G.; King, P. W. *J. Am. Chem. Soc.* **2012**, *134*, 5627.
(38) Wang, F.; Wang, W.-G.; Wang, X.-J.; Wang, H.-Y.; Tung, C.-H.; Wu, L.-Z. *Angew. Chem., Int. Ed.* **2011**, *50*, 3193.
(39) Zhu, H.; Song, N.; Lv, H.; Hill, C. L.; Lian, T. *J. Am. Chem. Soc.* **2012**, *134*, 11701.
(40) (a) Wang, F.; Liang, W.-J.; Jian, J.-X.; Li, C.-B.; Chen, B.; Tung, C.-H.; Wu, L.-Z. *Angew. Chem., Int. Ed.* **2013**, *52*, 8134. (b) Li, C.-B.; Li, Z.-J.; Yu, S.; Wang, G.-X.; Wang, F.; Meng, Q.-Y.; Chen, B.; Feng, K.; Tung, C.-H.; Wu, L.-Z. *Energy Environ. Sci.* **2013**, *6*, 2597.
(41) Wu, K.; Chen, Z.; Lv, H.; Zhu, H.; Hill, C. L.; Lian, T. *J. Am. Chem. Soc.* **2014**, *136*, 7708.
(42) Shemesh, Y.; Macdonald, J. E.; Menagen, G.; Banin, U. *Angew. Chem., Int. Ed.* **2011**, *50*, 1185.
(43) McNamara, W. R.; Han, Z.; Yin, C.-J.; Brennessel, W. W.; Holland, P. L.; Eisenberg, R. *Proc. Natl. Acad. Sci. U. S. A.* **2012**, *109*, 15594.
(44) Sproules, S.; Wieghardt, K. *Coord. Chem. Rev.* **2010**, *254*, 1358.
(45) Sproules, S.; Kapre, R. R.; Roy, N.; Weyhermüller, T.; Wieghardt, K. *Inorg. Chim. Acta* **2010**, *363*, 2702.
(46) Sellmann, D.; Geck, M.; Moll, M. *J. Am. Chem. Soc.* **1991**, *113*, 5259.
(47) Begum, A.; Sarkar, S. *Eur. J. Inorg. Chem.* **2012**, *2012*, 40.
(48) Fontecilla-Camps, J. C.; Volbeda, A.; Cavazza, C.; Nicolet, Y. *Chem. Rev. (Washington, DC, U. S.)* **2007**, *107*, 4273.
(49) Shima, S.; Pilak, O.; Vogt, S.; Schick, M.; Stagni, M. S.; Meyer-Klaucke, W.; Warkentin, E.; Thauer, R. K.; Ermler, U. *Science* **2008**, *321*, 572.
(50) Armstrong, F. A.; Belsey, N. A.; Cracknell, J. A.; Goldet, G.; Parkin, A.; Reisner, E.; Vincent, K. A.; Wait, A. F. *Chem. Soc. Rev.* **2009**, *38*, 36.
(51) Mulder, D. W.; Shepard, E. M.; Meuser, J. E.; Joshi, N.; King, P. W.; Posewitz, M. C.; Broderick, J. B.; Peters, J. W. *Structure* **2011**, *19*, 1038.
(52) Gunsalus, I. C.; Barton, L. S.; Gruber, W. *J. Am. Chem. Soc.* **1956**, *78*, 1763.
(53) Talapin, D. V.; Mekis, I.; Götzinger, S.; Kornowski, A.; Benson, O.; Weller, H. *J. Phys. Chem. B* **2004**, *108*, 18826.
(54) Evans, D. F. *J. Chem. Soc.* **1959**, 2003.
(55) Josef, P. US Patent No. US2842578, 1958.
(56) Bruker; *SADABS V2008-1*, BRUKER AXS Inc.: Madison, WI, 2008.
(57) Bruker; *SAINT, V8.27b*, BRUKER AXS Inc.: Madison, WI, 2012.
(58) Altomare, A.; Burla, M.; Camalli, M.; Cascarano, G.; Giacovazzo, C.; Guagliardi, A.; Moliterni, A.; Polidori, G.; Spagna, R. *SIR97: A new program for solving and refining crystal structures*; Istituto di Cristallografia, CNR: Bari, Italy, 1999.
(59) Sheldrick, G. *Acta Crystallogr., Sect. A: Found. Crystallogr.* **2008**, *64*, 112.
(60) Daifuku, S. L.; Al-Afyouni, M. H.; Snyder, B. E. R.; Kneebone, J. L.; Neidig, M. L. *J. Am. Chem. Soc.* **2014**, *136*, 9132.
(61) Kanatzidis, M. G.; Coucouvanis, D. *Inorg. Chem.* **1984**, *23*, 403.
(62) Kang, B. S.; Weng, L. H.; Wu, D. X.; Wang, F.; Guo, Z.; Huang, L. R.; Huang, Z. Y.; Liu, H. Q. *Inorg. Chem.* **1988**, *27*, 1128.
(63) Ray, K.; Bill, E.; Weyhermüller, T.; Wieghardt, K. *J. Am. Chem. Soc.* **2005**, *127*, 5641.
(64) Ray, K.; Begum, A.; Weyhermüller, T.; Piligkos, S.; van Slageren, J.; Neese, F.; Wieghardt, K. *J. Am. Chem. Soc.* **2005**, *127*, 4403.
(65) Birchall, T.; Greenwood, N. N. *J. Chem. Soc. A* **1969**, *0*, 286.
(66) Jasieniak, J.; Califano, M.; Watkins, S. E. *ACS Nano* **2011**, *5*, 5888.
(67) Weinberg, D. J.; He, C.; Weiss, E. A. *J. Am. Chem. Soc.* **2016**, *138*, 2319.
(68) Aldana, J.; Lavelle, N.; Wang, Y.; Peng, X. *J. Am. Chem. Soc.* **2005**, *127*, 2496.
(69) Jia, Y.; Chen, J.; Wu, K.; Kaledin, A.; Musaev, D. G.; Xie, Z.; Lian, T. *Chem. Sci.* **2016**, *7*, 4125.

DOI: 10.1021/jacs.6b05040
J. Am. Chem. Soc. 2016, 138, 11654−11663